



Molecular Crystals and Liquid Crystals

Publication details, including instructions for authors and subscription information:

<http://www.tandfonline.com/loi/gmcl16>

smectic Phase Structures of CVyano-Dicyclohexyl Liquid Crystals

E. Rahimzadeh^a, T. Tsang^a & L. Yin^{b a}

^a Department of Physics, Howard University, Washington, D.C., 20059

^b NASA Goddard Space Flight Center, Greenbelt, Maryland, 20771

Version of record first published: 20 Apr 2011.

To cite this article: E. Rahimzadeh, T. Tsang & L. Yin (1986): smectic Phase Structures of CVyano-Dicyclohexyl Liquid Crystals, *Molecular Crystals and Liquid Crystals*, 139:3-4, 291-298

To link to this article: <http://dx.doi.org/10.1080/00268948608080134>

PLEASE SCROLL DOWN FOR ARTICLE

Full terms and conditions of use: <http://www.tandfonline.com/page/terms-and-conditions>

This article may be used for research, teaching, and private study purposes. Any substantial or systematic reproduction, redistribution, reselling, loan, sub-licensing, systematic supply, or distribution in any form to anyone is expressly forbidden.

The publisher does not give any warranty express or implied or make any representation that the contents will be complete or accurate or up to date. The accuracy of any instructions, formulae, and drug doses should be independently verified with primary sources. The publisher shall not be liable for any loss, actions, claims, proceedings, demand, or costs or damages whatsoever or howsoever caused arising directly or indirectly in connection with or arising out of the use of this material.

Smectic Phase Structures of Cyano-Dicyclohexyl Liquid Crystals

E. RAHIMZADEH and T. TSANG

Department of Physics, Howard University, Washington, D.C. 20059

and

L. YIN

NASA Goddard Space Flight Center, Greenbelt, Maryland 20771

(Received January 2, 1986; in final form February 17, 1986)

The smectic phase structures of *p*-ethyl- and *p*-butyl-*p*'-cyanocyclohexyl-cyclohexane (ECCH and BCCH) have been found to be quite different from each other despite the similarities in molecular structures. The former structure is close to rhombohedral with $a = b = c = 12.5 \text{ \AA}$, $\alpha = \beta = \gamma = 28^\circ$ and one molecule per unit cell. In contrast, the latter structure is close to hexagonal close-packed with $a = b = 5.7 \text{ \AA}$ and $c = 31 \text{ \AA}$ and two molecules per unit cell. Since intermolecular forces may be quite weak in these systems, it appears that crystal structure can change considerably even though molecular structure is only slightly altered. An X-ray image intensification device (the Lixiscope) is helpful in the search for symmetric diffraction patterns.

p-Alkyl-*p*'-cyanocyclohexyl-cyclohexane, $R(C_6H_{10})(C_6H_{10})CN$, is a new class of liquid crystals where R may be any alkyl (C_nH_{2n+1}) group.^{1,2} One or both cyclohexane ($-C_6H_{10}-$) rings may also be replaced by phenyl ($-C_6H_4-$) rings. In the present work, we have determined the smectic phase structures of *p*-ethyl- and *p*-butyl-*p*'-cyanocyclohexyl-cyclohexane (ECCH and BCCH), $C_2H_5(C_6H_{10})(C_6H_{10})CN$ and $C_4H_9(C_6H_{10})(C_6H_{10})CN$. Despite the similarities in these two molecular structures, we have found quite different crystal structures with different crystal symmetries, due perhaps to the rather weak interactions between the cyclohexane ring systems.³

Because of the weak intermolecular forces in BCCH and ECCH, and because of the absence of magnetic susceptibility anisotropies as

compared to the phenyl compounds, it is difficult to align the molecules by external magnetic or electric fields. We are able to obtain single-domained samples in capillary tubes by slow cooling (~ 0.1 deg/min) from the less-ordered nematic phase at higher temperatures. Nevertheless, the spatial orientation of the domain inside the capillary depends on the direction of the initial nucleation and is therefore rather arbitrary. With the sample mounted on a goniometer, we have found it convenient to use an X-ray image intensification device (the Lixiscope) to search for symmetric diffraction patterns visually while the goniometer is rotated.

In the Lixiscope,^{4,5} the diffracted X-rays are converted into visible light images by a rare-earth scintillation phosphor. The visible light output is then coupled via fiber optics to a microchannel-plate image intensifier which intensifies the visible light signal with a luminous gain of $\sim 10^5$. Because of the high luminous gain, the intensified visible light output can be viewed directly, photographed, or coupled to other video devices. The transmission Laue spots on the output screen of the Lixiscope can be easily viewed in subdued room light while the sample is being rotated. Hence this is a convenient technique to study liquid crystals such as ECCH or BCCH whose molecular alignment inside the sample capillary is not known.

The X-rays are produced by a copper-anode tube with a nickel filter, usually operated at 22 kV and 500 Watts. After collimation, the horizontal X-ray beam is directed onto the liquid crystal sample which is placed in a thin-walled capillary tube installed on a two-axis goniometer. The goniometer is enclosed in a container so that the sample may be heated or cooled in an air stream with controlled temperature. The Lixiscope, which is small and compact, is placed in the forward scattering direction about 4 cm from the sample. The diffraction pattern displayed on the Lixiscope output screen can be recorded by a Polaroid camera. Calibration of the Lixiscope and camera recording is accomplished by placing standard lead grids (with circular and with rectangular grid patterns) over the scintillation screen. The linear resolution of the Lixiscope is about 0.2 mm, giving an angular resolution of about 0.3° .

For any spot formed by the scattered X-ray beam at the co-latitude angle 2θ and azimuthal angle ϕ_e (subscript *e* for experimental) in the spherical coordinate system, its reciprocal lattice vector \mathbf{G} may be expressed in terms of the unit vectors \hat{x} , \hat{y} , \hat{z} of the laboratory coordinate system:

$$\mathbf{G} = (4\pi \sin\theta/\lambda)(\hat{x} \cos\theta \cos\phi + \hat{y} \cos\theta \sin\phi - \hat{z} \sin\theta)$$

where \hat{z} is the direction of the incident X-ray beam, λ is the X-ray wave length, and θ is the Bragg angle. The first and the second parentheses are the magnitude and the unit vector respectively. The angle ϕ differs from the experimental angle ϕ_e by 180° because the Lixiscope presents an inverted image. It should be noted that the diffraction spots can come from both the characteristic $\text{CuK}\alpha$ radiation ($\lambda = 1.54 \text{ \AA}$) and the white radiations with shorter wave lengths from the copper anode. The former spots tend to have higher intensities. These two types of spots may be more clearly distinguished by lowering the X-ray voltages. A lowered voltage would lead to much larger reductions in the intensities of the white radiation spots as compared to the $\text{CuK}\alpha$ radiation spots. We also note that only the directions (but not the magnitudes) of the \mathbf{G} -vectors may be obtained from the diffraction spots produced by the white radiation.

Because of the low crystalline orders and large molecular fluctuations in liquid crystals, diffraction spots are observable only in the forward direction with small θ . It is therefore necessary to measure several diffraction patterns for various goniometer orientations and then express the \mathbf{G} -vectors for these different goniometer orientations in terms of a common set of unit vectors which is arbitrarily fixed in the crystal.

For the smectic phase of ECCH at 32°C , we have searched and found a diffraction pattern with threefold symmetry as sketched in Figure 1a. The photograph of the Lixiscope output is shown as Figure 2. The bright spots, denoted as a , b , c , have the same value of $2\theta = 16.8^\circ$ and form an equilateral triangle where the values of ϕ_e are 120° apart. These spots come from the $\text{CuK}\alpha$ radiation and remain bright even when the X-ray tube voltage is reduced to 20 kV or less. The X-ray direction is coincident with the direction of the threefold axis. The three bright spots may be assigned to the primitive reciprocal lattice vectors \mathbf{A} , \mathbf{B} , \mathbf{C} . Their magnitudes have the common value of 1.19 \AA^{-1} . The translation vectors \mathbf{a} , \mathbf{b} , \mathbf{c} for the unit cell are calculated from $\mathbf{a} = 2\pi(\mathbf{B} \times \mathbf{C})/(\mathbf{A} \cdot \mathbf{B} \times \mathbf{C})$, etc. These data suggest a rhombohedral unit cell with $|\mathbf{a}| = |\mathbf{b}| = |\mathbf{c}| = 12.5 \text{ \AA}$ and the common angle of 28° between pairs of these lattice vectors. The vectors \mathbf{a} , \mathbf{b} , \mathbf{c} are 17° away from the threefold axis direction. It should be noted that while it would be difficult to fulfill the Bragg conditions perfectly and simultaneously for all three lattice points \mathbf{a} , \mathbf{b} , \mathbf{c} at the $\text{CuK}\alpha$ wave length, it is quite likely that the sample is near the Bragg condition for a "perfect" crystal. Consequently, the smectic disorder can project the images of these lattice points onto the Lixiscope and their values are probably close to the actual values.

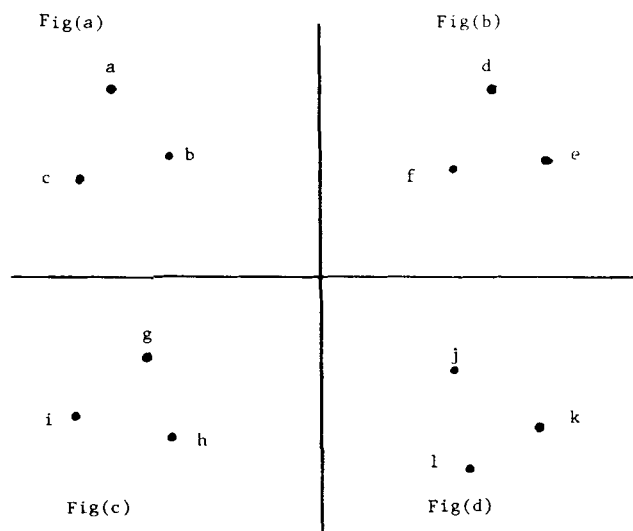


FIGURE 1 Sketch of diffraction patterns of smectic phase of ECCH from $\text{CuK}\alpha$ X-rays. (a) X-ray beam along threefold axis; (b)(c)(d) X-ray beam 16° away from the threefold axis and 120° apart azimuthally.

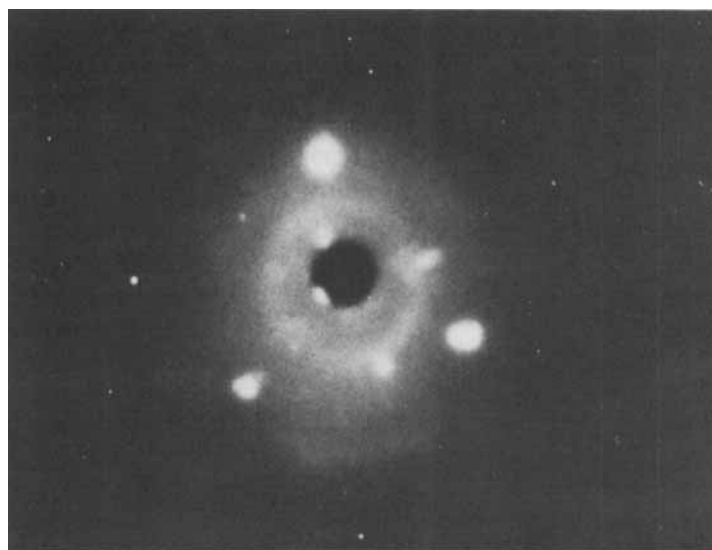


FIGURE 2 Photograph of Lixiscope output for smectic phase of ECCH with X-ray along the threefold axis (same as Figure 1a).

At other goniometer angles, the diffraction patterns sketched in Figure 1b, 1c, 1d have been observed. They are quite similar to each other. In contrast to Figure 1a, the X-ray directions for these patterns are tilted about 16° from the threefold axis and are distributed symmetrically about the threefold axis. In Figure 1b, the spots *d*, *e*, *f* occur at $2\theta = 16.8^\circ$ and the experimental *G*-vectors correspond very closely to $-\mathbf{B} - \mathbf{C}$, $-\mathbf{A} - \mathbf{B}$ and \mathbf{B} for the $\text{CuK}\alpha$ radiation. As expected from the threefold symmetry, very similar diffraction patterns were found in Figure 1c and 1d. These spots remain bright even when the X-ray tube voltage is reduced below 20 kV.

These results indicate that the smectic phase of ECCH is close to rhombohedral with $a = b = c = 12.5 \text{ \AA}$, crystallographic angles of $\alpha = \beta = \gamma = 28^\circ$ and unit cell volume of 395 \AA^3 . It is interesting to point out that rhombohedral structures are rather uncommon for the smectic phases of liquid crystals. Very similar diffraction patterns have also been observed for the entire temperature range of the smectic phase of ECCH. With one molecule per unit cell, the unit cell volume is consistent with our density measurement of 0.96 gr/cm^3 , which corresponds to a unit cell volume of 379 \AA^3 . The ECCH molecular shape is known to be approximately cylindrical, with a length of 14 \AA and a diameter of 6 \AA . From the smectic phase structure, the intermolecular distance is found to be $(2a)\sin(\alpha/2) = 6.0 \text{ \AA}$ within the molecular plane perpendicular to the threefold axis. It is seen that this intermolecular distance is the same as the ECCH molecular diameter. Because of the slight staggering of molecules along the threefold axis, the unit cell edge of 12.5 \AA and the distance of $12.5\cos 17^\circ = 12.0 \text{ \AA}$ between molecular planes are both slightly shorter than the ECCH molecular length of 14 \AA .

It is surprising to find that the smectic phase structure (at 29°C) of BCCH is quite different from ECCH despite the similarities in their molecular structures. Again, we used the Lixiscope to search for symmetric diffraction patterns. These patterns are sketched in Figure 3, and the Lixiscope photographs are shown in Figure 4. A pattern of sixfold symmetry is found for a freshly prepared sample, as shown in Figure 3a. The bright diffraction spots (due to $\text{CuK}\alpha$ radiation) occur at $2\theta = 18.1^\circ$ with approximately equal intensities. Their azimuthal angles are 60° apart, indicating that the X-ray beam is parallel to the sixfold axis. These *G*-vectors may be written as linear combinations of $\pm\mathbf{A} + \mathbf{C}$, $\pm\mathbf{B} + \mathbf{C}$, and $\mp\mathbf{A} \pm \mathbf{B} + \mathbf{C}$ of the reciprocal lattice vectors of the hexagonal cell. These spots remain bright even when the X-ray tube voltage is reduced to 20 kV or less. From Figure 3a, we obtained $|\mathbf{A}| = |\mathbf{B}| = 1.27 \text{ \AA}^{-1}$ and $|\mathbf{C}| = 0.20 \text{ \AA}^{-1}$. The

Figure (a)

Figure (b)

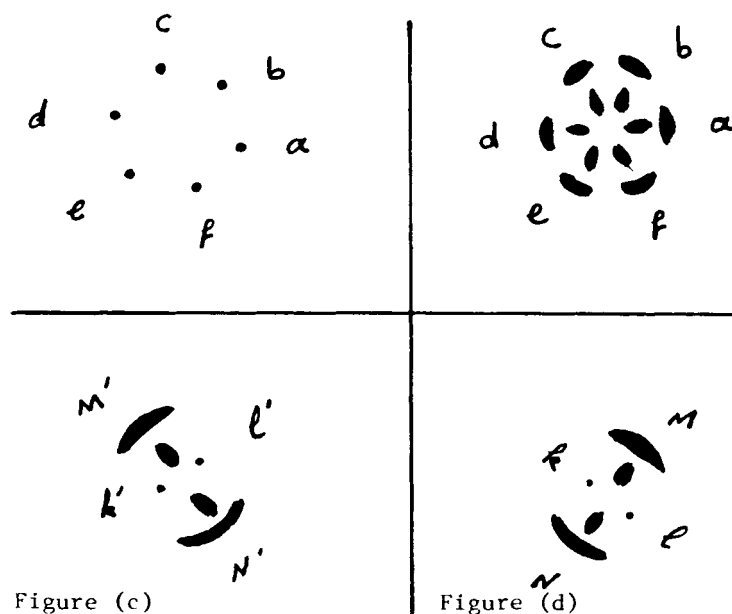


FIGURE 3 Sketches of diffraction patterns of smectic phase of BCCH from CuK α X-rays. (a) X-ray beam along sixfold axis, freshly prepared sample; (b) X-ray beam along sixfold axis, one-day old sample; (c)(d) X-ray beams perpendicular to sixfold axis, 60° apart from each other.

magnitudes of these vectors are $4\pi/(3^{1/2}a)$, $4\pi/(3^{1/2}b)$, and $2\pi/c$, where a , b , c are the hexagonal unit cell parameters. Thus we get $a = b = 5.7 \text{ \AA}$ and $c = 31 \text{ \AA}$. We found that the sixfold diffraction pattern became broader for a sample about a day after its preparation, as shown in Figure 3b. This broadening may be due to the development of substantial variations in the tilt of the BCCH molecules with respect to the c -axis.

Changing the goniometer angles resulted in a pattern with twofold symmetry as sketched in Figure 3c. The Lixiscope photograph is shown as Figure 4c. For this pattern, the X-ray direction is perpendicular to both C (the sixfold axis direction) and B . The spots k' and l' at $2\theta = 5.8^\circ$ correspond very closely to $\mp 2C$. Similarly, m' and n' at $2\theta = 18^\circ$ correspond very closely to $\pm B$. All of these come from CuK α radiation and remain bright even when the X-ray tube voltage is reduced to 20 kV or less. The sharp spots k' and l' are in direct contrast to the rather broad crescents m' and n' . These differences

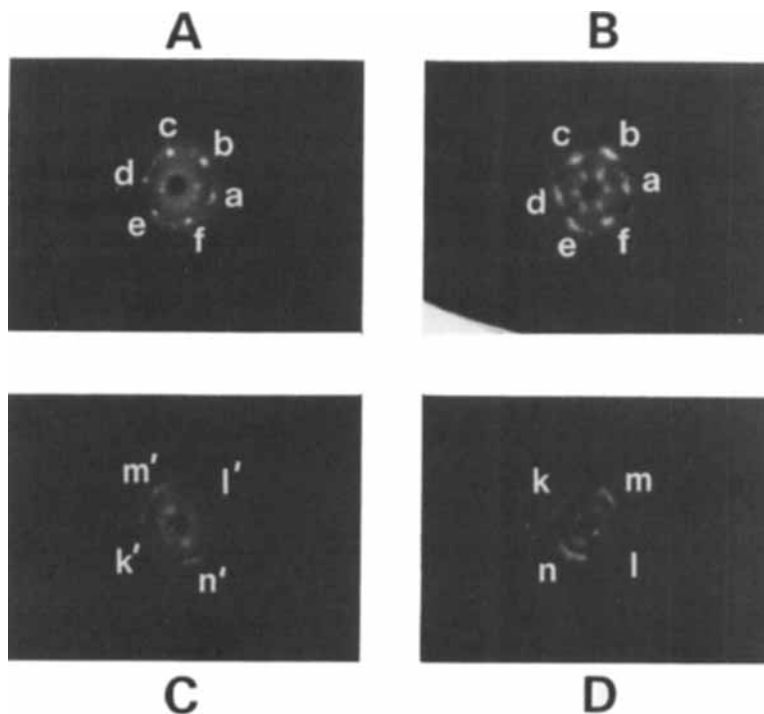


FIGURE 4 Lixiscope output photographs of diffraction patterns of smectic phase of BCCH corresponding to Figures 4a to 4d.

suggest that there may be good long-range order parallel to the c -axis but not perpendicular to the c -axis. There may also be some tilt of BCCH molecules with respect to the c -axis. A very similar pattern is sketched in Figure 3d and the Lixiscope photograph is shown as Figure 4d. For this pattern, the X-ray direction is still perpendicular to C but is 60° away from the previous X-ray direction used in Figure 3c. Again, the spots k, l (at $2\theta = 5.8^\circ$) and the crescents m, n (at $2\theta = 18^\circ$) correspond very closely to $\mp 2C$ and $\mp A \pm B$. The streaks near the center of the photographs come from white radiation; they would disappear when the X-ray tube voltage is reduced to 20 kV or less.

These results indicate that the smectic phase structure of BCCH is close to hexagonal with $a = b = 5.7 \text{ \AA}$, $c = 31 \text{ \AA}$, and a unit cell volume of $3^{1/2}a^2c = 870 \text{ \AA}^3$. Our density measurement of 0.97 gr/cm^3 gives the volume per molecule as 430 \AA^3 . Hence there are two BCCH molecules per unit cell. Such hexagonal close-packed structures with two molecules per unit cell have also been observed for the smectic phases of several other liquid crystals.⁶⁻⁸ For the smectic phase of

BCCH, the unit cell parameter a is nearly the same as the molecular diameter while the parameter c is slightly less than twice the molecular length.

These experiments indicate that the liquid crystal structures in the smectic phase can change considerably even when their molecular structures are only slightly different. For BCCH and ECCH, this phenomena may be a consequence of the weak intermolecular forces in cyclohexane ring systems.³ These experiments also serve to illustrate the potential usefulness of the Lixiscope and other image intensification devices in X-ray diffraction studies of liquid crystals.

The partial financial support by the National Aeronautical and Space Administration grant NAG-5-156 is gratefully acknowledged.

References

1. L. Pohl, R. Eidenschink, J. Krause and D. Erdmann, *Phys. Lett.*, **60A**, 421 (1977).
2. L. Pohl, R. Eidenschink, J. Krause and G. Weber, *Phys. Lett.*, **65A**, 169 (1978).
3. S. K. Burley and G. A. Petsko, *Science*, **229**, 23 (1985).
4. L. Yin, J. I. Trombka and S. M. Seltzer, *Nucl. Instrum. Methods*, **158**, 175 (1979).
5. L. Yin, J. I. Trombka and S. M. Seltzer, *Nucl. Instrum. Methods*, **172**, 471 (1980).
6. I. G. Chistyakov, *Adv. Liq. Cryst.*, **1**, 143 (1975).
7. G. R. Luckhurst and G. W. Gray, *The Molecular Physics of Liquid Crystals*, Academic Press, New York, 1979.
8. J. Prost, *Adv. Phys.*, **33**, 1 (1984).